Les Rencontres Scientifiques de l'IFP - Advances in Hybrid Powertrains - 25-26 November 2008 - Proceedings

ON THE USE OF GENETIC ALGORITHM TO OPTIMIZE THE ON-BOARD ENERGY MANAGEMENT OF A HYBRID SOLAR VEHICLE

Ivan Arsie, Raffaele Di Martino, Gianfranco Rizzo, Marco Sorrentino*

Department of Mechanical Engineering, University of Salerno, 84084 Fisciano (SA), Italy,
msorrentino@unisa.it
** Corresponding author*

Abstract — ON THE USE OF GENETIC ALGORITHM TO OPTIMIZE THE ON-BOARD ENERGY MANAGEMENT OF A HYBRID SOLAR VEHICLE — *This paper deals with the development of a prototype of Hybrid Solar Vehicle (HSV) with series structure. This activity has been also conducted in the framework of the EU funded Leonardo project "Energy Conversion Systems and Their Environmental Impact", a project with research and educational objectives. A study on supervisory control for hybrid solar vehicles and some preliminary tests performed on the road are presented. Previous results obtained by a model for HSV optimal design have confirmed the relevant benefits of such vehicles with respect to conventional cars in case of intermittent use in urban driving (city-car), and that economical feasibility could be achieved in a near future. Due to the series-powertrain adopted for the HSV prototype, an intermittent use of the ICE powering the electric generator is possible, thus avoiding part-load low-efficient engine operations. The best ICE power trajectory is determined via genetic algorithm optimization accounting for fuel mileage as well as battery state of charge, also considering solar contribution during parking mode. The experimental set up used for data logging, real-time monitoring and control of the prototype is also presented, and the results obtained with different road tests discussed.*

INTRODUCTION

Sustainable Mobility issues are gaining increasing attention both among specialists and in public opinion, due to the major impact of automotive systems on carbon dioxide production, climate changes and fossil fuel depletion. Recently, increasing efforts are being spent towards the application of solar energy to electric and hybrid cars. While solar vehicles do not represent a practical alternative to cars for normal use, the concept of a hybrid electric car assisted by solar panels appears more realistic [1].

In fact, thanks to a relevant research effort, in the last decade Hybrid Electric Vehicles (HEV) have evolved to industrial maturity, and represent now a realistic solution to important issues, such as the reduction of gaseous pollution in urban drive as well as the need for a substantial increase of energy conversion efficiencies. On the other hand, the use of solar energy on cars has been considered with a certain skepticism by most users, including automotive engineers. This may be due to the simple observation that the net power achievable in a car with current photovoltaic panels is about two order of magnitude less than maximum power of most of today cars. But a more careful analysis of the energy involved demonstrate that this perception may be misleading. In fact, there is a large number of drivers utilizing daily their car for short trips and with limited power demand [2]. In those conditions, the solar energy collected by solar panels on the car along a day may represent a significant fraction of the energy required for traction [3].

In spite of their potential interest, solar hybrid cars have received relatively little attention in literature. Some prototypes have been developed or are under current development [4]. Although these works demonstrate the general feasibility of such an idea, detailed presentation of results and performance, along with a systematic approach to solar hybrid vehicle design, seem still missing in literature.

Therefore, appropriate methodologies are required to address both the rapid changes in the technological scenario and increasing availability of innovative, more efficient components and solutions. A specific difficulty in developing a Hybrid Solar Vehicle relates to the many mutual interactions between energy flows, powertrain balance of plant and sizing, vehicle dimension, performance, weight and costs, whose connections are much more critical than in either conventional or hybrid electric vehicles. Moreover, the control strategies for HSV cannot be simply derived from the solutions developed for HEV. In fact, the presence of solar panels requires to extend the SOC management strategies also to parking phases, while the study of suitable control techniques is needed in order to maximize the net power

from solar panels [5]. Finally, many HSV prototypes tend to adopt a series structure, while most of today HEV adopt a parallel or series/parallel approach. Series structure appears more suitable for plug-in hybrid applications [6], and is compatible with the use of in-wheel motors with built-in traction control and anti-skid [7]. Moreover, the series configuration represents a natural bridge towards the introduction of fuel cell hybrid vehicles.

This paper deals with modeling, on-board energy management and performance evaluation for a prototype of Hybrid Solar Vehicle with series structure. This activity has been started in the framework of the UE funded Leonardo project "Energy Conversion Systems and Their Environmental Impact" [8], a project with research and educational objectives.

1 THE HSV PROTOTYPE

Table I lists the main features and specifications of the HSV prototype (see Figure 1), now under-development at DIMEC-UNISA lab facilities.

Table 1: Actual HSV prototype specifications.

Vehicle	**Piaggio Porter**
Length	3.370 m
Width	1.395 m
Height	1.870 m
Drive ratio	1:4.875
Electric Motor	**BRUSA MV 200 – 84 V**
Continuous Power	9 KW
Peak Power	15 KW
Batteries	**16 6V Modules Pb-Gel**
Mass	520 Kg
Capacity	180 Ah
Photovoltaic Panels	**Polycrystalline**
Surface A_{PV}	1.44 m^2
Weight	60 kg
Efficiency (including converter)	0.1
Electric Generator	**Yanmar S 6000**
Power COP/LTP	5.67/6.92 kVA
Weight	120 kg
Overall weight (w driver)	
M_{HSV}	1950 kg

Vehicle lay-out is organized according to a series hybrid architecture, as shown on Figure 2. With this approach, the photovoltaic panels PV (placed on vehicle roof as shown on Figure 1) assist the Electric Generator EG, powered by an Internal Combustion Engine (ICE), in recharging the Battery pack (B) in both parking mode and driving conditions, through the Electric Node (EN). The Electric Motor (EM) can either provide the mechanical power for the propulsion or restore part of the braking power during regenerative braking. In this structure, the thermal engine can work mostly at constant power, corresponding to its optimal efficiency, while the electric motor EM is designed to assure the attainment of the vehicle peak power.

Figure 1: The Hybrid Solar Vehicle Prototype.

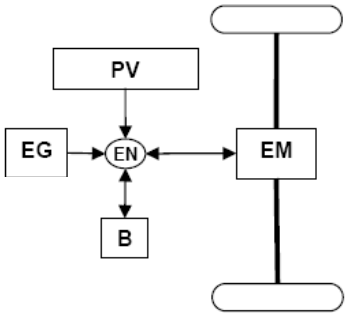

Figure 2: Scheme of the series hybrid solar vehicle.

2 HSV MODELING AND EXPERIMENTAL CHARACTERIZATION

HSV simulation, whose results are presented in Section 4, was performed by means of a longitudinal vehicle model developed under the following hypotheses: i) drag (C_x) and rolling (C_r) coefficients are assumed equal to 0.4 and 0.02, respectively; ii) the drag force is considered acting on vehicle centre of gravity; iii) overall transmission efficiency η_{tr} is set to 0.9; iv) rotational inertia is accounted for increasing vehicle weight by 10%, therefore effective mass M_{eff} equals 1.1 M_{HSV}. The resulting longitudinal model relates requested power at wheels to the road load, as follows:

$$P_w = M_{HSV} \cdot g \cdot v \cdot [C_r \cos(\alpha) + \sin(\alpha)] + 0.5 \rho C_x A v^3 + + M_{eff} \frac{dv}{dt} v \quad (1)$$

where α and v are the road grade and vehicle speed, respectively. For non negative P_w values, the mechanical power requested to the EM is:

$$P_{EM} = \frac{P_w}{\eta_{tr}} \qquad if \quad P_w \geq 0 \tag{2}$$

P_{EM} can also be expressed as function of power contributions coming from electric generator, battery and PV array, as follows:

$$P_{EM} = \eta_{EM}\left(P_{EG} \cdot \eta_{AC/DC} + P_B + P_{PV}\right) \quad if \quad P_w \geq 0 \tag{3}$$

where P_x is the power supplied by the x component (i.e. electric generator, battery and photovoltaic panels), η_{EM} is the EM efficiency and $\eta_{AC/DC}$ is the AC/DC converter efficiency, here set to 0.92.

On the other hand, when P_w<0, the regenerative braking mode is active, resulting in the following expression for the electrical energy delivered by the EM:

$$P_{EM} = P_w \cdot \eta_{tr} \cdot \eta_{EM} \qquad if \quad P_w < 0 \tag{4}$$

During regenerative braking, battery can be charged by EG and PV also, thus the following equation holds for negative P_w values:

$$P_B = P_{EM} - P_{EG} \cdot \eta_{AC/DC} - P_{PV} \quad if \quad P_w < 0 \tag{5}$$

2.1 Electric generator

The electric generator, is composed of a Diesel engine, one cylinder, 406 cm^3, coupled with a 3 phase synchronous induction machine. Experiments were carried out to map the efficiency of the electric generator in a wide operating region, accounting for the whole path from fuel to electrical power. The experimental set-up was arranged with a 3-phase pure resistive, balanced electrical load. The measurements were accomplished at constant engine speed (3000 rpm), corresponding to a 50 Hz electric signal, with regularly spaced variation of electrical load by steps of 600 W, up to 5400 W. Figure 3 shows the experimental EG efficiency vs. the output power of the electrical generator (EG). The efficiency was detected by processing the measurements of fuel consumption and output voltage and current, as follows:

$$\eta_{EG} = \frac{P_{EG}}{\dot{m}_f H_i} = \frac{V \cdot I}{\dot{m}_f H_i} \tag{6}$$

In Figure 3 the efficiency predicted by a black box model identified vs. the experimental data is also plotted. The model expresses the overall efficiency of the electric generator as function of the output electrical power by a 4th order polynomial regression.

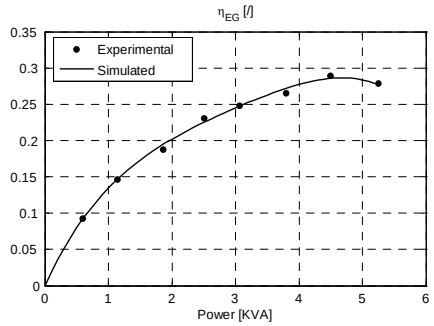

Figure 3: Comparison between experimental and predicted electric generator efficiency.

2.2 PV array

Regarding the PV energy contribution to vehicle traction, it was computed on the basis of real energy measurements collected on a stationary PV plant located within UNISA area. The measured energy distribution results in the following daily average evaluated on a year basis:

$$E_{sun,day} = 3.1 \qquad \left[\frac{kWh}{kWp\,day}\right] \tag{7}$$

Considering the PV roof efficiency of 10%, a nominal power of 1kW can be obtained with a 1/0.1=10 m^2 array. Therefore, daily average energy yielded by the 1.44 m^2 PV roof (see Table 1) can be estimated as follows:

$$E_{PV} = E_{sun,day} \cdot \frac{A_{PV}}{10} = 3.1 \cdot \frac{1.44}{10} = 450 \quad [Wh/day] \tag{8}$$

2.3 Battery pack

The battery pack model estimates battery state of charge (SOC), current and thermal state as function of the actual electrical power (i.e. positive in discharge and negative in charge). The actual current is computed starting from the electrical power, by applying the Kirchoff's law to the equivalent circuit shown on Figure 4. The internal resistance R_{in} was modeled, following the approach proposed by [9], as a nonlinear function of battery temperature and state of charge. Figure 5 focuses on the effect of SOC, showing high charge and discharge resistance at high and low SOC, respectively.

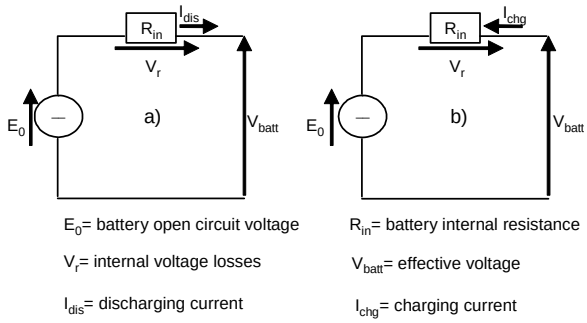

Figure 4: Equivalent circuit of the battery pack [a) discharge; b) charge].

The battery model accuracy was checked by comparing simulated data with experiments conducted both in case of battery discharging and charging (see Figure 6). The agreement between experiments and model outputs confirms the validity of extending the model proposed by [9] to the battery pack the HSV prototype is equipped with. It is worth mentioning that the data shown in Figure 6 refer to initial SOC values of 1 and 0.6 for battery discharging and charging, respectively.

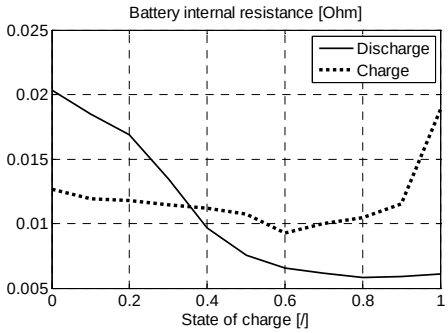

Figure 5: Variation of battery internal resistance in charging and discharging as function of SOC [9].

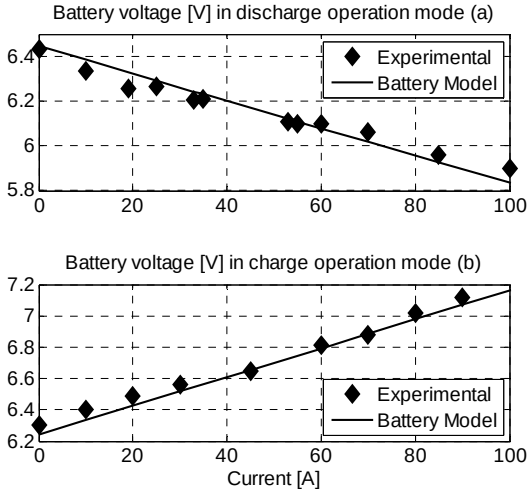

Figure 6: Comparison between model [9] and experimental data collected during battery discharging and charging.

2.4 Electric motor

The efficiency of the electric motor (EM) is simulated by a black box model identified vs. the technical data sheets provided by motor manufacturer. The model expresses the efficiency as function of the mechanical power provided for the propulsion via a 3rd order polynomial regression. Figure 7 shows both experimental and simulated efficiency vs. provided power.

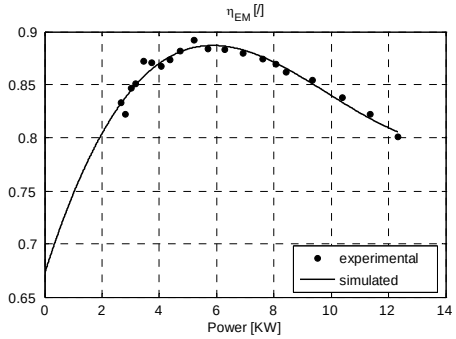

Figure 7: Comparison between experimental and predicted electric motor efficiency vs. provided power.

3 OPTIMAL ENERGY MANAGEMENT ON HSV VEHICLES

Hybrid Solar Vehicles have of course many similarities with Hybrid Electric Vehicles, for which many studies on the optimal management and control of energy flows have been presented in last years [10–14]. Nevertheless, the presence of solar panels and the adoption of a series structure may require to study and develop specific solutions for optimal management and control of an HSV.

In fact, in most electric hybrid vehicles a charge sustaining strategy is adopted: at the end of a driving path, the battery state of charge should remain unchanged. With a solar hybrid vehicle, a different strategy should be adopted as battery is charged during parking hours as well. In this case, a different goal can be pursued, namely restoring the initial state of charge within the end of the day rather than after a single driving path [15].

Moreover, the series configuration suggests quite an efficient solution, namely to operate the engine in an intermittent way at constant operating conditions. Of course, the maximum gain in terms of fuel consumption occurs when the EG power corresponds to the most efficient value. In such case, the engine-generator system may be designed and optimized to maximize its efficiency, emissions and noise at design point, while in current automotive engines the maximum efficiency is usually sacrificed to the need of assuring stable

operation and good performance in the whole operating range.

In order to develop a supervisory control to be implemented on the vehicle, a more accurate analysis of the optimal EG power distribution over an arbitrary driving cycle has to be performed. This task is discussed in the next sub-section.

3.1 Optimization of electric generator scheduling by means of genetic algorithms

The optimal EG power trajectory can be found by solving the following constrained optimization problem.

$$\min_X \int \dot{m}_{f,HSV}(X)dt \tag{9}$$

subject to the constraints:

$$\Delta SOC_{day} = SOC_f - SOC_0 + \Delta SOC_p = 0 \tag{10}$$

$$SOC > SOC_{\min} \tag{11}$$

$$SOC < SOC_{\max} \tag{12}$$

where $\dot{m}_{f,HSV}$ is the HSV fuel consumption [kg], SOC_f and SOC_0 are the initial and final state of charge in the driving phase, respectively, and ΔSOC_p is the SOC increase due to PV recharging during vehicle parking. The decision variables X include number of EG-on events N_{EG}, along with corresponding starting time $t_{0,EG,i}$, duration $\Delta_{t,EG,i}$ and EG power level $P_{EG,i}$, where i is the i-th EG-on event.

The first constraint (Eq. 10) allows to restore the initial state of charge within the end of the day, also considering parking phases.

It is worth noting that the proposed energy management strategy is based on the knowledge of the vehicle route. Future activities will focus on the extension of the optimization outcomes to different driving scenarios as well as insolation conditions.

The other constraints (i.e. Eqs. 11and 12) were defined accounting for internal resistance dependence on battery state of charge. Figure 5 shows that in the SOC range [0.55 0.9] both charging and discharging resistances are fairly constant while being close to their minimum values. Therefore in this analysis SOC_{min} and SOC_{max} were set to 0.55 and 0.9, respectively.

The problem stated by Eqs. (9) through (12) involves both integer (e.g. N_{EG}) and real variables, thus falling in the field of Mixed Integer Programming (MIP) problems. Among the several techniques that can be adopted to solve such problems, genetic algorithms (GA) is one of the most efficient [16] and has thus been selected for optimizing EG scheduling on the HSV prototype.

The GA search was performed in Matlab environment by means of the GAtbx tool developed by [17]. GA optimization consists of an iterative procedure that can be schematized as follows:

Phase 1: an initial population of N_{ind} individuals (or solutions) representing the search domain (i.e. the decision variables domain) is generated randomly.

Phase 2: An objective function F is evaluated for each individual. Then, assuming that a minimization task is being accomplished, all the individuals are ranked in ascending order on the basis of their F_k value. This way the so-called "fitness" is assigned to the k-th individual, whose value will range from a maximum to a minimum depending on its rank position.

Phase 3: Fitness-based selection of best individuals. According to the evolutionary theory, the best individuals have the highest probability to join the next population. The "Roulette Wheel" and "Stochastic Universal Sampling" [17] are among the most widely adopted techniques to perform a random selection of the strongest individuals as function of their fitness. Particularly, the higher its fitness is, the more likely that individual will be selected. In this work, the latter method was applied.

Phase 4: Generation of new individuals. Phase 3 usually yields a new set of individuals containing a higher number of "strong" (i.e. with high fitness) solutions, whereas some of the weakest ones disappear. This intermediate set undergoes a renewal process consisting of two different steps: crossover and mutation. The former step basically makes a certain number of individual pairs, selected randomly, to exchange part of their genotype with each other. The resulting genotypes will of course behave differently in the next population, thus yielding a couple of new individuals. After crossover, mutation takes place, once again based on random selection of some individuals.

It is worth mentioning that an elitist approach is usually followed in Phase 4, in that some of the strongest individuals from the current population are ensured to be present in the next one. This way, even though a lower number of off-springs is introduced, the best solutions from the current population are preserved [17].

Phase 2 through Phase 4 are repeated as many times as the desired number of new generations is reached. The above description highlights the need for the decision maker to select several operating parameters (Nind, crossover and mutation probabilities, number of

generations) depending on problem complexity and computational time requirements. Further details about GA optimization techniques can be found in the abundant literature on the topic, which the reader is addressed to [16–19].

For the current application, the following operating parameters were assumed:

Table 2 – GA operating parameters.

N_{ind}	50
Number of generations	300
Crossover probability	0.7
Mutation probability	0.06

Regarding the binary representation to define the individual genotype, the number of bits per each decision variable was calculated according to the information provided in Table 3:

Table 3 – Binary representation of the optimization problem.

Decision variable	Definition range	Precision	Number of bits
N_{EG}	[1 4]	1	2
t_{EG} (min)	[0 53]	0.055	10
Δt_{EG} (min)	[0 53]	0.055	10
P_{EG} (kW)	[0 5.5]	0.0055	10

4 SCENARIO ANALYSIS

In order to assess the HSV prototype performance not only at the current developmental stage, but also analyzing two further scenarios of improved vehicle configurations, a simulation analysis was performed. Such an analysis was accomplished by solving, in a backward manner, the longitudinal vehicle dynamics (i.e. Eq. 1) for a driving cycle composed of 4 ECE cycles, as the one shown on Figure 8.

4.1 Results

Table 4 summarizes the results obtained in the three analyzed scenarios. Particularly, it emerges that an acceptable fuel economy can be obtained even with current vehicle configuration (i.e. scenario 1). This is possible thanks to the high efficient use of the Diesel engine addressed by the GA based optimization described above. Particularly, Figure 9 shows that the Diesel engine is turned on once, after 15 minutes, delivering 5 kW to battery and/or EM for about 25 minutes. This allowed to operate the EG itself at an overall efficiency as high as 0.28 (see Figure 3). The EG energy contribution caused battery to partially recover the state of charge reduction occurred in the first part of the driving cycle, resulting in a final SOC of 0.732, as shown on Figure 10. The lower value of SOC with respect to the initial one is in accordance with the constraint expressed by Eq. (10).

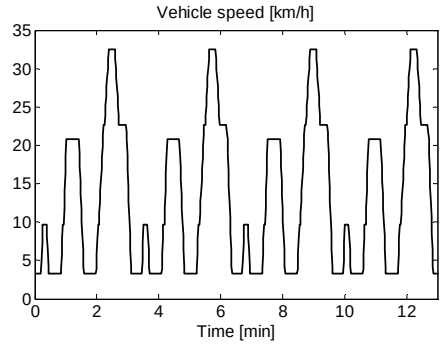

Figure 8: Module of ECE driving cycle.

Regarding the other scenarios, it is worth mentioning here that the second scenario corresponds to an optimized vehicle configuration, in which a 0.18 efficient PV array (i.e. E_{PV} = 810 Wh/day) replaces the actual one and battery capacity is lowered down to 75 Ah. The latter hypothesis takes into account the impact of vehicle hybridization, as the added electric generator allows to reduce both battery storable energy and nominal power. The lower battery capacity also causes the weight to decrease from 1950 kg to 1658 kg. Such a configuration results in a fuel economy improvement up to 22 km/liter, as indicated in Table 4. Figure 11 shows that in scenario 2 the optimal EG scheduling addressed by the GA optimization consists of two EG-on events and lower average EG power with respect to scenario 1, which in turn results in a lower energy contribution by the EG. This is linked to the lower final SOC to be reached at the end of the driving phase (see Figure 10) as compared to scenario 1. The low final SOC (about 0.675) is due to the higher amount of solar energy and the lower battery capacity simulated in scenario 2. In conclusion, both weight reduction and PV efficiency increase contribute to achieve the fuel economy improvement. Particularly, the fuel saving is equivalent to 0.2 liter in the reference transient and is due by 56% to weight reduction and by 44% to PV efficiency.

Finally, the third scenario was considered to account for a further weight reduction (i.e. 20%), obtainable by improving vehicle materials [3]. The simulated fuel economy in this case gets close to 30 km/liter. As in scenario 2, the final SOC sets to 0.675, as shown on Figure 10. On the other hand, the energy contribution requested to the EG is further low as compared to scenario 2, due to the lower vehicle weight assumed in scenario 3. In order to maximize fuel economy, this time the GA optimization yielded a solution with 3 EG-on events, each one with shorted duration than scenario 2 but similar average power, as shown on Figure 11.

Table 4 – HSV simulation results.

Scenario	1	2	3
η_{PV}	0.1	0.18	0.18
Battery capacity (Ah)	180	75	75
M_{hsv}	1950	1658	1326
Fuel economy (km/liter)	15.18	21.70	29.15

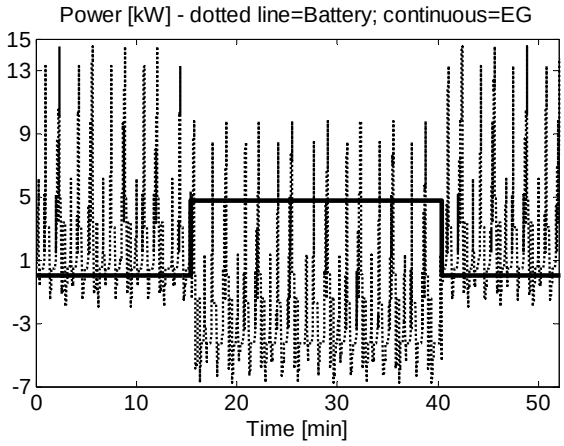

Figure 9: EG and battery power trajectories for scenario 1.

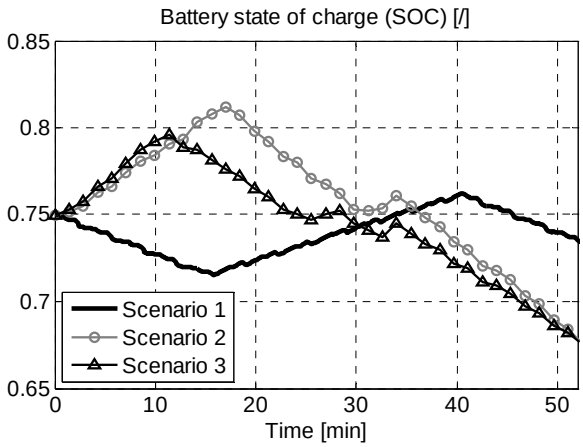

Figure 10: SOC trajectories for all simulated scenarios.

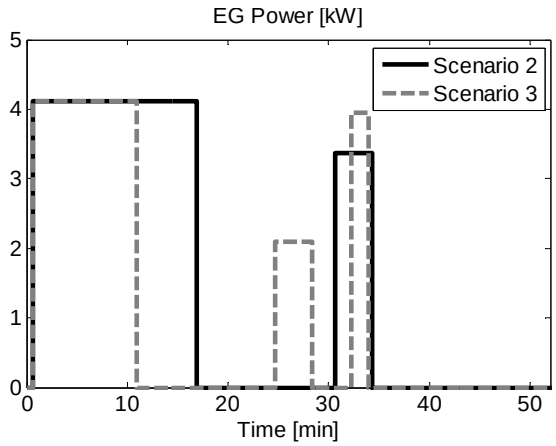

Figure 11: EG power trajectories for scenarios 2 and 3.

5 MEASUREMENT SYSTEM ON THE VEHICLE

The prototype has been equipped with a measurement system for real-time monitoring and data logging. Two experiments have been also carried out using different road tests. Schematically, the measure chain is reported in Fig.12.

Moreover, the measurement system Ni C-Rio provides the acquisition vehicle torque while the solar prototype is running. A scheme of these measurements is shown in Fig. 13.

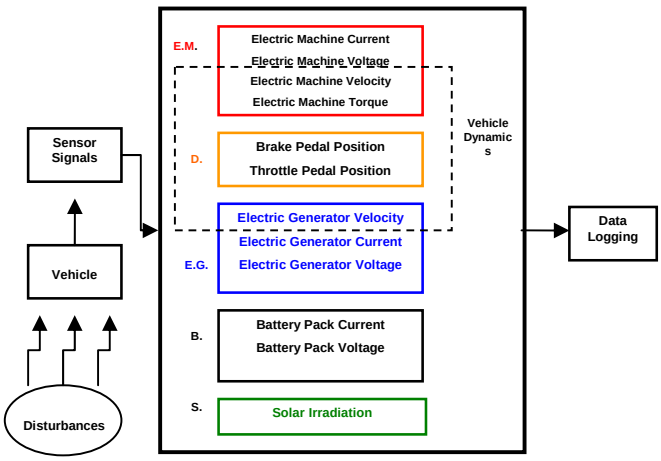

Fig. 12 – Schematic representation of the acquisition system.

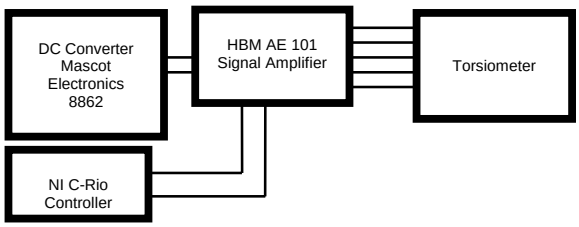

Fig. 13 – Measurement Scheme carried out for the torque real-time monitoring.

5.1 Experimental results on the vehicle

Some preliminary on-road tests were performed to measure the electric current in different vehicle conditions.

Fig. 14 shows the brake and traction maneuvers imposed during the first test. As expected, when the driver brakes (e.g. at approximately 25 seconds in Fig. 14 (a)) the electric machine switches to generator operation, thus charging the battery pack with current down to -50 Amps (see Fig. 14 (b)). Then, when the driver presses the accelerator pedal, the current sudden increases above 300 Amps for few seconds, before decaying towards steady-state operation (i.e. around 100 Amps), as shown on Fig. 14 (b).

The on-going activity is directed to the completion of the vehicle measurement system, in order to perform a detailed validation of vehicle dynamic models. Other data have been collected during acceleration-deceleration maneuvers (Fig. 15) and for slope-up and slope-down maneuvers (Fig.16).

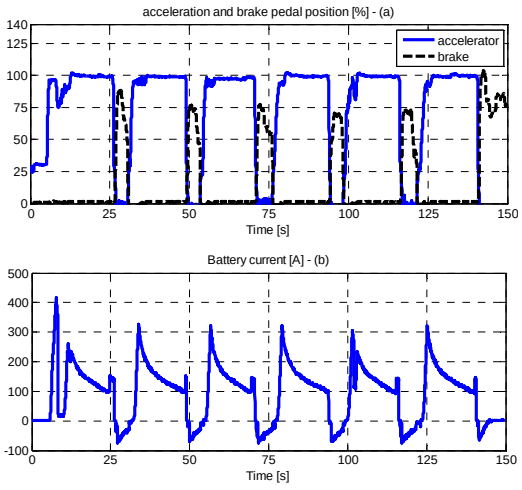

Fig. 14 – Experimental results collected in the first road test.

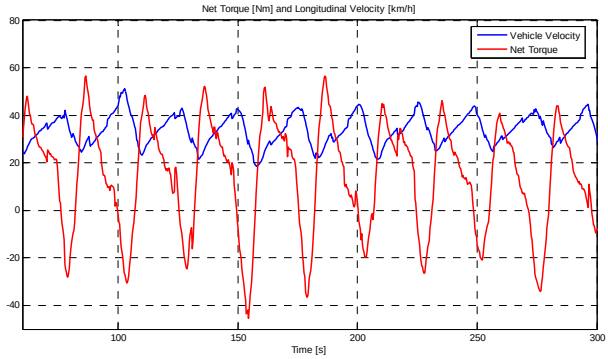

Fig. 15 – Experimental results collected in the second road test.

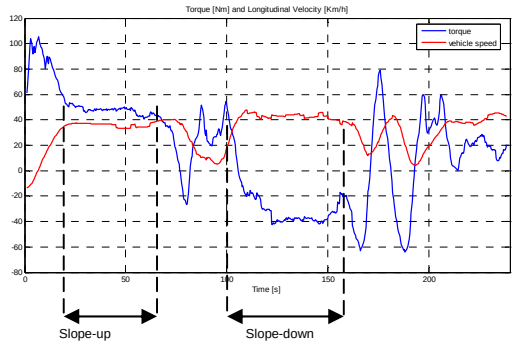

Fig. 16 – Experimental results collected in the third road test.

6 CONCLUSIONS

The paper reported on the actual developmental stage of a hybrid solar vehicle prototype. The experimental and numerical activities conducted to develop and validate a comprehensive HSV model were presented. The model accounts for vehicle longitudinal dynamics along with the accurate evaluation of energy conversion efficiency for each powertrain component.

Genetic algorithm optimization was proposed to address some of the most challenging issues in the development of hybrid solar vehicles with series structure, namely the definition of the optimal electric generator scheduling.

Actual vehicle performance and fuel economy were analyzed by simulating the HSV prototype on a driving route composed of 4 ECE cycles. The resulting fuel consumption was 15 km/liter. Further simulations showed that fuel economy can be increased up to 30 km/liter both by substituting the actual PV array with more advanced solar technology and by appropriately resizing HSV components.

On-going and future activities focus on numerical, experimental and prototype developmental tasks. Particularly, the procedure proposed to define the optimal EG scheduling via genetic algorithm optimization will be extended to optimal energy management of HSV in presence of varying insolation and lack of a-priori knowledge of driving route. In parallel, suited on the-road test and measurements will be performed to validate both simulation results and control strategies effectiveness. Regarding prototype improvements, the installation of an automated sun-tracking roof to further enhance solar energy captation is under current study.

ACKNOWLEDGMENTS

The authors would like to acknowledge the European Union, the Italian Ministry of University and Research and the University of Salerno for their support to the research activity presented in this paper.

REFERENCES

1. Neil C., 2006, “Solar Hybrid Vehicles”, Energy Pulse, available at www.energypulse.net.
2. Statistics for Road Transport, available at www.statistics.gov.uk/CCI/nscl.asp? ID=8100.
3. Arsie I., Marotta M., Pianese C., Rizzo G., Sorrentino M., 2005, “Optimal Design of a Hybrid Electric Car with Solar Cells”, Proc. of 1st AUTOCOM Workshop on Preventive and Active Safety Systems for Road Vehicles, Istanbul, Sept.19-21.
4. Fiat Phylla, 2008, www.motorauthority.com/ cars/fiat/fiat-phylla-concept-previews-new-topolino-electric-minicar/.
5. Petrone, G., Femia, N., Spagnuolo, G., Vitelli M., 2005, “Optimization of perturb and observe maximum power point tracking method”, IEEE Transactions on Power Electronics. Vol. 20, pp. 963-973.
6. Letendre S., Perez R., Herig C., 2003, “Vehicle Integrated PV: A Clean and Secure Fuel for Hybrid Electric Vehicles”, Proc. of the American Solar Energy Society Conference, June 21-23, Austin,TX.
7. www.itee.uq.edu.au/~serl/UltraCommuter.html.
8. Leonardo Program “Energy Conversion Systems and Their Environmental Impact”, http://www.dimec.unisa.it/leonardo.
9. Burch, S., Cuddy, M., Johnson, V., Markel, T., Rausen, D., Sprik, S., Wipke, K., "ADVISOR: Advanced Vehicle Simulator", available at http://www.avl.com/advisor.
10. Powell, B.K., Bailey, K.E., Cikanek, S.R., 1998, “Dynamic modeling and Control of Hybrid Vehicle Powertrain Systems”, IEEE Trans.Contrl Syst., vol. 18, no. 5, 1998.
11. Baumann, B., Rizzoni, G., Washington, G., 1998, “Intelligent Control of Hybrid Vehicles using Neural Networks and Fuzzy Logic”, SAE paper 981061.
12. Guzzella L., Amstutz, A., 1999, “CAE Tools for Quasi-Static Modeling and Optimization of Hybrid Poweretrains”, IEEE Transactions on Vehicular Technology, vol. 48, no. 6, November 1999.
13. Arsie, I., Graziosi, M., Pianese, C., Rizzo, G., Sorrentino, M., 2005, “Optimization of Supervisory Control Strategy for Parallel Hybrid Vehicle with Provisional Load Estimate”, JSAE Review of Automotive Engineering, Vol. 26, No. 3, pp. 341-348, 2005.
14. Arsie, I., Di Martino, R., Rizzo, G., Sorrentino, M., 2008, “Energy Management for a Hybrid Solar Vehicle with Series Structure”, Proc. of the 17th IFAC World Congress, July 6-11, 2008, Seoul, Korea.
15. Arsie, I., Rizzo, G., Sorrentino, M., 2007, “Optimal Design and Dynamic Simulation of a Hybrid Solar Vehicle”, SAE paper 2006-01-2997, SAE Transactions – Journal of Engines, vol. 115-3.
16. Sakawa, M., Kato, K., Ushiro, S., Inaoka, M., 2001, “Operation planning of district heating and cooling plants using genetic algorithms for mixed integer programming”, Applied Soft Computing Vol.1, pp. 139–150.
17. Chipperfield, A.J., Fleming, P.J., Polheim, H., Fonseca, C.M., “Genetic Algorithm Toolbox – Matlab Tutorial”, Department of Automatic Control and System Engineering - University of Sheffield, downloadable at http://www.shef.ac.uk/acse/research/ecrg/getgat.html.
18. Chipperfield, A.J., Fleming, P.J., Fonseca, C.M., 1994, “Genetic Algorithm Tools for Control Systems Engineering”, Proc. Adaptive Computing in Engineering Design and Control, Plymouth Engineering Design Centre, 21-22 September, pp. 128-133, 1994.
19. Zitzler, E., 1999, “Evolutionary Algorithms for Multiobjective Optimization: Methods and Applications”, Ph.D. Thesis, ETH Swiss Federal Institute of Technology, Zurich, Switzerland.